Nanostructure of Polyplexes Formed between Cationic Diblock Copolymer and Antisense Oligodeoxynucleotide and Its Influence on Cell Transfection Efficiency

XiuBo Zhao,[†] Fang Pan,[†] ZhuoQi Zhang,[†] Colin Grant,[†] YingHua Ma,[‡] Steven P. Armes,[‡] YiQing Tang,[§] Andrew L. Lewis,[§] Thomas Waigh,[†] and Jian R. Lu*[,†]

Biological Physics, School of Physics and Astronomy, The University of Manchester, Oxford Road, Manchester M13 9PJ, United Kingdom, Department of Chemistry, Dainton Building, The University of Sheffield, Brook Hill, Sheffield, South Yorkshire S3 7HF, United Kingdom, and Biocompatibles UK Ltd., Farnham Business Park, Farnham, Surrey GU9 8QL, United Kingdom

Received June 10, 2007; Revised Manuscript Received August 25, 2007

Although various cationic polymers have been used to condense anionically charged DNA to improve their transfection efficiency, there is still a lack of fundamental understanding about how to control the nanostructure and charge of the polyplexes formed and how to relate such information to cell transfection efficiency. In this work, we have synthesized a weak cationic and phosphorylcholine-containing diblock copolymer and used it as a model vector to deliver an antisense oligodeoxynucleotide (ODN) into HeLa cells. Small angle neutron scattering (SANS) was used to determine the copolymer/ODN polyplex structure. The SANS data revealed the formation of polyplex nanocylinders at high copolymer (N)/ODN (P) charge ratios, where N symbolizes the amine groups on the copolymer and P symbolizes the phosphate groups. However, the cylindrical lengths remained constant, indicating that the ODN binding over this region did not alter the cylindrical shape of the copolymer in solution. As the N/P ratio decreased and became close to unity the polyplex diameters remained constant, but their lengths increased substantially, suggesting the end-to-end bridging by ODN binding between copolymer cylinders. As the N/P ratios went below unity (with ODN in excess), the polyplex diameters increased substantially, indicating different ODN bridging to bundle the small polyplexes together. Transfection studies from HeLa cells indicated a steady increase in transfection efficiency with increasing cationic charge and decreasing polyplex size. Cell growth inhibition assay showed significant growth inhibition by the polyplexes coupled with weak cytotoxicity, indicating effective ODN delivery. While this study has confirmed the overall charge effect, it has also revealed progressive structural changes of the polyplexes against varying charge ratio, thereby providing useful insight into the mechanistic process behind the ODN delivery.

Introduction

Gene delivery has great potential to cure many genetic and acquired diseases. Non-viral gene delivery is especially advantageous because it could avoid unacceptable immune responses and other adverse events as recently reported for viral gene delivery.[1−4] However, the main obstacle to non-viral gene delivery is its low gene transfection efficiency, caused by the poor transport of DNA across cell membranes[2] and the subsequent decomplexation of the transfecting vector from DNA after internalization. Various cationic polymers have shown promising effects in facilitating gene delivery as they readily complex with DNA to form polyplexes by neutralizing the negatively charged anionic phosphate groups and hence improve transfection.[5−16] Cationic polymers such as poly-L-lysine (PLL), poly(ethyleneimine) (PEI), and polyamidoamine dendrimers all readily form complexes with DNA through electrostatic interaction. Modified natural polymers such as chitosan and its derivatives are also widely used, but they are usually polydisperse and require careful control of charge density, making it difficult to link their structural properties to gene transfection. The polymers used to date for complexation are diverse and vary in size, molecular architecture, and chemical nature, so there is still a lack of understanding to guide the design of polymer structure to match a given DNA and cell type for optimal performance.

However, research in non-viral gene delivery has advanced so drastically over the past few years that a number of polymer-based cell transfection reagents have become commercially available. Further research is needed to rationalize the relationship between polymeric molecular architecture, the structure of polymer/DNA complexes formed, and their physiochemical properties such as solubility and charge character. This work will then help develop a useful knowledge base for linking our molecular understanding to cell transfection efficiency and cytotoxicity, with due consideration of differences arising from different cells.[1,15,17−19]

Diblock copolymers, especially those containing cationic and hydrophilic segments, offer the benefit of electrostatic complexation while enhancing the solubility and stability of the polyplexes.[1,10,20] Insertion of hydrophilic segments such as PEO (poly(ethylene) oxide) into diblock copolymers provides a hydrophilic corona that creates a steric barrier against self-aggregation, shielding of cationic charged groups, and inhibits the association with plasma proteins and other cellular components.[17−19] In contrast to the work on PEO copolymer

* To whom correspondence should be addressed. Tel.: 0044-161-3063926. E-mail: j.lu@manchester.ac.uk.
[†] The University of Manchester.
[‡] The University of Sheffield.
[§] Biocompatibles UK Ltd.

10.1021/bm7006482 CCC: $37.00
Published on Web 10/16/2007

Scheme 1. Representative Chemical Structure of the MPC-Tertiary Amine Methacrylate Diblock Copolymers, Where R Denotes Ethyl Groups

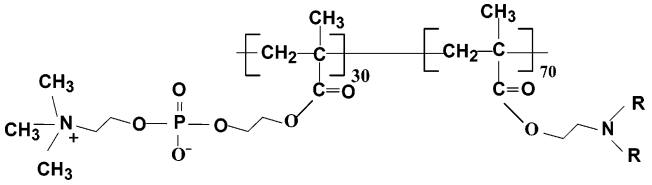

vectors, we have designed a weak cationic diblock copolymer, MPC30−DEA70 (where MPC refers to 2-(methacryloyloxy)-ethyl phosphorylcholine and DEA refers to 2-(diethylamino)-ethyl methacrylates; 30 and 70 refer to the mean degrees of polymerization of each block), to highlight the main structural features of solution complexation between the copolymers and antisense oligodeoxynucleotides (ODNs). The molecular structure of the copolymer is shown in Scheme 1. MPC segments are zwitterionic and strongly hydrated, and they provide hydrophilic affinity for the polyplexes to remain soluble while the charge density is varied over a wide range. Unlike PEO segments, however, the extent of hydration of PC groups shows little response to temperature or ionic strength. MPC-based polymers have shown excellent bio- and hemo-compatibility and have been used as coating materials for various medical implants such as contact lenses, guidewires, ear grommets, and coronary stents.[20−23] Their application as gene transfecting vectors represents a novel exploitation of their advantageous biocompatibility in non-viral gene delivery. The incorporation of cationic DEA segments provides uniform tertiary charges and a simpler molecular architecture than the widely used PEI segments (containing different charge types and often more complex molecular structures).

ODNs are normally 12−25 nucleotides in length.[5,24] They could either hybridize with specific mRNA through the Watson−Crick base pair complementarity to form duplexes, which would inhibit the transcription of genetic information into protein synthesis, or activate the RNase H that can digest the mRNA, thus resulting in the blockade of the pathway.[5,24−28] As ODNs can significantly inhibit cell proliferation by sequence-specific down-regulation of gene expression, they have applications in cancer therapy, coronary in-stent restenosis, and other types of gene functionalization.[10,24,25,29−31] Antisense technology has been widely studied in the past decade with extensive effort devoted to the modification of the antisense ODN's chemical structure such as methylphosphonate and phosphorothioate ODNs and sequence design.[5,7,26] However, their benefits can only be realized when viable approaches for efficient delivery of the ODNs into cells have been developed.[4,6,8,11,27,28]

For transgenic expression to occur, therapeutic DNA molecules have to overcome a set of intracellular barriers.[1,32,33] A simple addition of ODNs into tissue culture or a bodily system does not transfer a sufficient amount of ODNs into most cell types.[27] Because of the poor internalization and ineffective antisense action of naked ODNs,[5,7,27,28] extensive research has been devoted to the identification and assessment of suitable vectors and mechanistic interactions.[4−6,8,27] These studies have revealed a wide range of transfection efficiencies from different vectors, but further understanding from these studies is hindered by the complexity in structure and composition of the vectors and the lack of direct information of solution nanostructure of ODN polyplexes. Powerful techniques such as scanning probe microscopy (SPM) and X-ray scattering and diffraction are often performed on polyplex powders, and the information may bear little relevance to interactions under physiological conditions. In this study, the small angle neutron scattering (SANS) experiments have been undertaken from the same solutions as used in cell transfection, focusing on the assessment of the effect of charge ratios between cationic amine groups and anionic phosphate groups in ODN (the N/P ratios) on the size and shape of the polyplexes formed. The SANS results have revealed a fascinating evolution of the cylindrical polyplexes with their initial diameters close to that of the single diblock copolymer at the high N/P ratio, indicating the binding of ODN to individual copolymers. As the copolymer content decreased and the N/P ratio approaches unity, the polyplex diameters remained constant, but their lengths showed substantial increases, indicating end-to-end bridging. Further decreases in copolymer concentration led to an increase in polyplex diameters, indicating the occurrence of cross-bundling between small polyplexes to form large ones. The size increase was concurrent with the decline of net positive charge density of these complexes. These variations have led to a steady decline in cell transfection efficiency.

Experimental Section

Materials. The synthesis of the diblock copolymer MPC30−DEA70 has been described previously.[34] The MPC block was first synthesized using atom transfer radical polymerization (ATRP) in methanol at 20 °C, and the 2-(diethylamino)ethyl methacrylate (DEA) monomer was then added to produce further chain growth. Stock MPC30−DEA70 copolymer solution was made by dissolving 0.1 g of copolymer in 10 mL of UHQ water (Purelab UHQ, Vivendi Water Systems Ltd.) or D_2O (SIGMA, UK, 99+ %D). The sample was then stirred overnight and subsequently diluted to the desired concentrations before use. The samples were filtered with 0.20 μm syringe filters. Single-stranded human c-myc antisense oligodeoxynucleotides (ODNs) (5′-AAC-GTT-GAG-GGG-CAT-3′, with and without 5′-FAM (carboxyfluorescein-5-succimidyl ester) labeled) were purchased from Eurogentec Ltd. (UK) and were HPLC purified. Oligofectamine transfection reagent was purchased from Invitrogen, UK.

Complex Fabrication. Copolymer/ODN complexes were made by adding the ODN solution to the copolymer solution. ODNs were dissolved in UHQ or D_2O and diluted to 1 mg/mL. The copolymer solution was diluted to the desired concentrations to achieve different cationic/anionic charge ratios (N/P ratios). Next, 300 μL of ODN solution was added to 300 μL of copolymer solution with mild shaking, and the sample was left to equilibrate for at least 30 min at room temperature before use. Thus, in all of the mixed solutions prepared, the ODN concentration was fixed at 0.5 mg/mL and the copolymer concentrations were varied between 0.3 (ca. 0.03 wt %) and 5 mg/mL (ca. 0.5 wt %) to achieve all of the N/P ratios required. All of the polyplexes were prepared at pH 7 and were studied by different physical methods under the same pH at 23−25 °C.

Agarose Gel Electrophoresis. Copolymer/ODN (without FAM labeling) complexes were prepared as described above. 2 μL complexes (1 μg DNA equivalence) for each sample were mixed with 1 μL of DNA loading buffer. They were then loaded into 1% agarose gel containing 0.50 μg/mL ethidium bromide (Sigma, UK). Electrophoresis was carried out at 100 V in 1 × TBE buffer (Tris-Borate-EDTA, Sigma, UK) for roughly 30 min. The ODN band was visualized under UV transillumination (Fisher, UK). Copolymers were stained by immersing the gel in coomassie blue staining solution consisting of 10% glacial acetic acid, 45% methanol, 45% UHQ, and 0.1% w/v coomassie bright blue G250 (Sigma, UK) for 30 min in a shaker followed by washing with destaining solution consisting of 10% glacial acetic acid, 10% methanol, and 80% UHQ overnight. Both of the pictures were captured by use of a Sony DSC T1 digital camera.

Dynamic Light Scattering (DLS). The principle of DLS is outlined by Berne et al.[35] DLS measures the intensity correlation function of

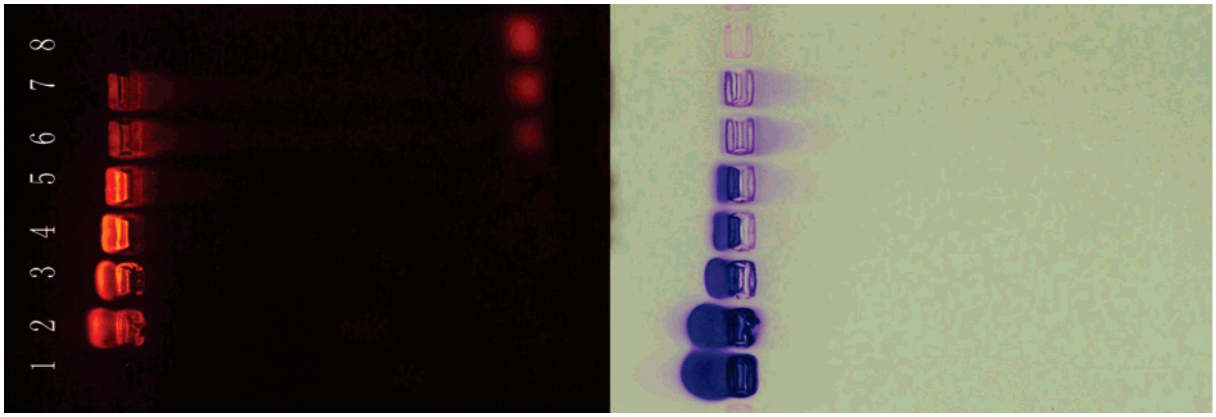

Figure 1. Agarose gel electrophoresis of MPC30−DEA70/ODN complexes. Lane 1 and lane 8 are copolymer and ODN controls. Lanes 2−7 correspond to 10:1, 5:1, 2:1, 1:1, 0.8:1, and 0.6:1 (N/P ratios), respectively. Left image shows the ODN migration by ethidium bromide stain; right image shows the copolymer migration by coomassie bright blue G250 stain.

light scattered from a polymeric solution. Analysis of the intensity correlation profiles provides the decay rate distribution from which the diffusion coefficient is determined. The Stokes−Einstein equation is then used to calculate the hydrodynamic radii of the pure copolymer and the polyplexes. All DLS measurements were performed using a Malvern Instruments NanoS Nanosizer. The instrument was fitted with a helium−neon laser (633 nm) with a size detection range from 0.6 nm to 6 μm. The detection angle was 173° with respect to the incoming beam. Samples analyzed were contained in a 1 cm path length quartz cell, and the data were analyzed using Malvern Instruments Dispersion Technology Software. The polymer refractive index was taken to be 1.45 with an absorbance of 0.001. The viscosity and refractive index of water were taken as 0.8872 cPa and 1.330, respectively. Six measurements were performed on each sample, with an average of 10 runs taken for each measurement, each within 1 min.

Small Angle Neutron Scattering (SANS). SANS has the required sensitivity to the size and shape of nanoparticles (pure polymer or the complexes) in solution. It has become a widely used technique in the characterization of polymers and proteins. The working principle of SANS and the outline of data treatment have been described by King.[36] The scattered intensity is due to the interaction of the neutron beam with a large number of nanoparticles and is sensitive to their volume, morphology (form factor), and distribution (interparticle structure factor). As the copolymer concentration used in this work was very low (typically <0.2 wt %), the interparticle factor was taken to be 1 in data analysis. D_2O was used as a solvent to provide the isotopic contrast. Otherwise, solutions were prepared in exactly the same way as for all other studies. SANS experiments were carried out at LOQ, ISIS Neutron Facility, Rutherford Appleton Laboratory (RAL), Oxford, UK, using neutron wavelengths ranging from 2.2 to 10 Å. The 64 cm square detector was at a distance of 4.1 m, giving a wave vector (κ) range of 0.006−0.28 $Å^{-1}$. Samples were contained in 2.0 mm path length fused silica cells. Data were corrected for the wavelength dependence of the incident spectrum, the measured sample transmission, and relative detector efficiencies, prior to subtraction of the respective D_2O buffer backgrounds. Absolute scaling was obtained by comparison with the scattering from a partially deuterated polystyrene standard. The data were fitted using the Fish2 program provided by RAL.

Atomic Force Microscopy (AFM). Complex solutions were deposited onto mica surfaces and dried in a vacuum oven for 2 min. The images were observed by Tapping Mode in isopropanol using the AFM microscope (Dimensions 3100 with a NanoScope IV controller from Veeco, Santa Barbara, CA) with 10 nm silicon nitride tips.

Cell Culture. HeLa cells (human cervical carcinoma cell line) were products from ATCC and were a gift from Dr. John Garland, Manchester Medical School, the University of Manchester, UK. The cells were cultured at 37 °C, 5% CO_2 in Dulbecco's Modified Eagle Medium (DMEM, Sigma, UK) supplemented with 10% heat-inactivated Fetal Bovine Serum (FBS, Sigma, UK), and 100 U/mL penicillin/50 mg/L streptomycin (Sigma, UK).

Cell Transfection and CLSM. Cells were seeded on cover glasses in 24-well plates at a density of 2×10^4 per well (in 1 mL of cell culture medium) and grown overnight at 37 °C, 5% CO_2. The cell culture medium was removed and then replaced (with and without 10% FBS). Copolymer/ODN complexes (0.5 μg ODN equivalence) formed at pH 7 and different N/P ratios were added into each well. Commercial Oligofectamine was used as positive controls following the instruction by the supplier. The ratio used was 3 μL of Oligofectamine to 1 μg of ODN. Also, ODN itself was used as negative controls. After 24 h incubation, the cells were washed with PBS (Sigma, UK) three times, then fixed with 4% paraformaldehyde (in PBS) for 5−10 min. They were then stained with 1 μM DAPI (4′,6-diamidino-2-phenylindole) for 10 min. ProLong Antifade reagent (Molecular Probes, UK) was used, and samples were analyzed using a fluorescent microscope (Leica, DM2500 M) and Leica SP2 CLSM (Leica, Germany). The number of both FAM-positive and DAPI-positive cells (representative for total cells) was recorded. The transfection efficiency was defined as the percentage of FAM-positive cells to the DAPI-stained total cell number.[37]

Cytotoxicity and Cell Growth Inhibition (MTT Assay). HeLa cells were seeded into 96-well cell culture plates at a density of 5×10^3 per well (in 200 μL of cell culture medium) and grown overnight at 37 °C, 5% CO_2, after which the medium was replaced as described above. Copolymer/ODN complexes at different N/P ratios (the amount of ODN was fixed at 0.1 μg/well) were added into each well, and the cells were incubated for 20 h. Different amounts of copolymer solutions (20 μL) equivalent to the dosages used for ODN complexes were also studied as parallel copolymer toxicity references. Oligofectamine was used as a positive control with ODN itself as a negative control. MTT (3-(4,5-dimethylthiazol-2-yl)-2,5-diphenyltetrazolium bromide) reagent (5 mg/mL, 20 μL/well) was then added into each well, and the cells were cultured for a further 4 h until the purple precipitate was visible. Purple precipitates in each well were then fully dissolved using 200 μL of DMSO (Sigma, UK) and measured at a wavelength of 570 nm with background subtraction at 650 nm by microplate reader (Sunrise Tecan, UK).

Results and Discussion

Agarose Gel Electrophoresis. The polyplexes formed through complexation between copolymer (N) and ODN (P) at different N/P ratios were first examined by agarose gel electrophoresis, and the main results are shown in Figure 1. All of the polyplexes formed were entirely soluble due to the presence of MPC blocks. As the copolymer and ODN carry opposite charges, the pure copolymer (lane 1) migrates to the opposite direction from the

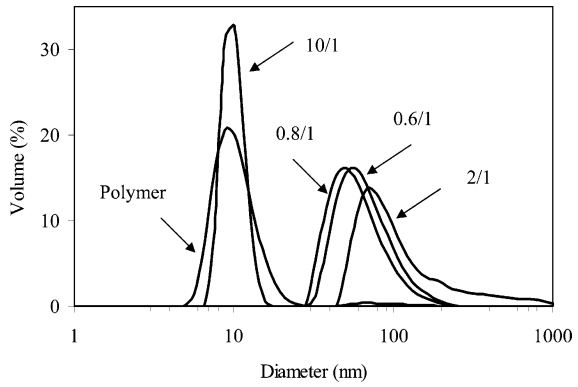

Figure 2. Dynamic light scattering (DLS) profiles of MPC30−DEA70 (5 mg/mL) and MPC30−DEA70/ODN (N/P) complexes at 10:1, 2:1, 0.8:1, and 0.6:1. ODN was fixed at 0.5 mg/mL for the complexes.

ODN (lane 8). However, the copolymer/ODN polyplexes migrate in both directions, depending on exact N/P ratios. The materials placed in lanes 2−4 correspond to high N/P ratios, and it can be clearly seen that some polyplexes are positively charged due to copolymer excess and move in the same direction as the pure copolymer. The sample wells are bright, indicating that some polyplexes are neutralized and stay in the wells. Lanes 5−7 show that, instead of a distinct DNA band of migration, a continuous retardation of the polyplexes is observed, indicating that the net charge density of the complexes is polydisperse. At N/P = 1 (lane 5), most polyplexes stay in the well due to the predominant charge neutrality, but a small fraction moves out, again indicating the polydispersity of the charge density. As the ODN is in excess (lanes 6 and 7), some polyplexes migrate to the same direction as the net ODN, indicating the net negative charges on these complexes. In addition, neat DNA bands are clearly visible in lanes 6 and 7, and, as the dosage of ODN was fixed at 1 μg/well, the more intensive ODN band in lane 7 indicates that fewer polyplexes were formed due to the lower amount of copolymer in sample 7. The gel plate study thus shows that the polyplexes formed bear a range of charge distribution. As the N/P ratio decreases, the charges on polyplexes show an overall trend of decrease and some of them become negatively charged. In all cases, a large fraction of polyplexes appears to stay charge-neutral.

Dynamic Light Scattering (DLS). DLS detects the mean dimension of nanoparticles in aqueous solution based on the Stocks−Einstein equation. The measurements were made on both pure copolymer and polyplexes using samples prepared under the same conditions as for gel electrophoresis. Figure 2 shows the representative volume intensity distribution profiles plotted against the hydrodynamic diameters, a measure of the mean dimension of the nanoparticles in solution. It can be seen from Figure 2 that the size from the pure copolymer has the peak around 10 nm. Mixing of ODN leads to the increase in the diameter, and as the concentration of copolymer decreases (a decrease in N/P ratio) the peaks move up and the distributions become broader. Thus, with ODN, the diameters being some 20 Å greater than that of the copolymer itself, the hydrodynamic diameter is similar to that of the pure copolymer. But at low N/P ratios (<2), the hydrodynamic diameter shows a substantial increase. There is also a substantial polydispersity in the hydrodynamic diameter from both pure copolymer and polyplexes. The polydispersity increases with decreasing N/P ratio, a trend broadly consistent with the charge distribution observed from gel electrophoresis.

DLS has been used extensively to probe the size changes from different DNA binding and complexation processes. For example, Hodrien et al.[38] have studied the binding of double-stranded herring testes DNAs (100 and 250 base pairs) onto amidine-functionalized polystyrene (PS) micro- and nanospheres and observed strong precipitation around charge neutrality. This is because in their systems solubilization was rendered by strong affinity of the charge groups to aqueous environment and when charge groups were neutralized precipitates formed. In our systems, the attachment of the zwitterionic block to the DEA block increased solubility and no precipitation was observed. In the work by Hodrien et al.,[38] there was an overall size increase with decreasing N/P ratio when DNA was bound to the small 10 nm PS particles. A similar trend can be seen from Figure 2. This observation shows that the same trend of size increase could be achieved by different sizes of DNA and that DNA charge excess must be the key factor.

Small Angle Neutron Scattering (SANS). SANS is sensitive to smaller length scales than DLS and is capable of revealing the shape of nanoparticles.[36] The polyplex solutions for SANS were again formed under the same conditions as used for electrophoresis and DLS, except in D_2O. The representative scattering profiles are shown in Figure 3 where a large change in the shape and level of the scattering profile against the N/P ratio can be seen. This trend of the shift of the scattering profile indicates the increase in aggregate size with decreasing copolymer concentration, consistent with the DLS observation shown in Figure 2.

SANS data analysis was started by testing different shapes such as sphere, disc, and cylinder with varying size. It was found that cylindrical shape was the only one appropriate to fitting all data measured, from both pure copolymer and polyplex solutions. The continuous lines shown in Figure 3 represent the best cylinder model fits, with different structural parameters listed in Table 1.

For the pure copolymer in 0.5 wt % solution, the best-fit cylinder corresponded to the diameter of 30 ± 2 Å and the length of 180 ± 30 Å. The fitting was more sensitive to changes in diameter but less so to the length variation. The errors quoted represented the ranges within which acceptable fits were produced. Thus, taking the experimental errors also from DLS, the hydrodynamic diameters obtained from DLS were close to the cylindrical lengths from SANS, showing good consistency between the two methods. Because the cross-sectional diameter for an average copolymer was around 30 Å, the diameters of the cylinders fitted were equivalent to the width of a single copolymer. As expected, the length of 180 ± 30 Å was shorter than the full extended length of 250 Å due to the flexibility of the methacrylate backbone.[39] The rigidity (B = contour length/end-to-end length = 1.38) is slightly lower than that expected for a standard polyelectrolyte such as poly(styrene sulfonate) ($B \approx 2-3$). Yet the increased rigidity as observed for the diblock copolymer might arise from the steric hindrance of the bulky pendant side groups in addition to the unscreened charges (extended electrostatic blobs).

Further SANS studies were made using copolymers at higher concentrations up to 2 wt % (data not shown). The same diameters of ca. 30 Å were observed, but the lengths showed a steady decrease against increasing copolymer concentration due to possible backbone bending. This part of the study shows that the MPC copolymer did not aggregate under the conditions studied. Instead, they existed in the form of free and stretched molecules.

Further SANS data analysis revealed that ODN binding at the N/P ratios of 10/1 and 5/1 resulted in the increase of the diameters of the polyplex cylinders from some 30 to 50 Å while

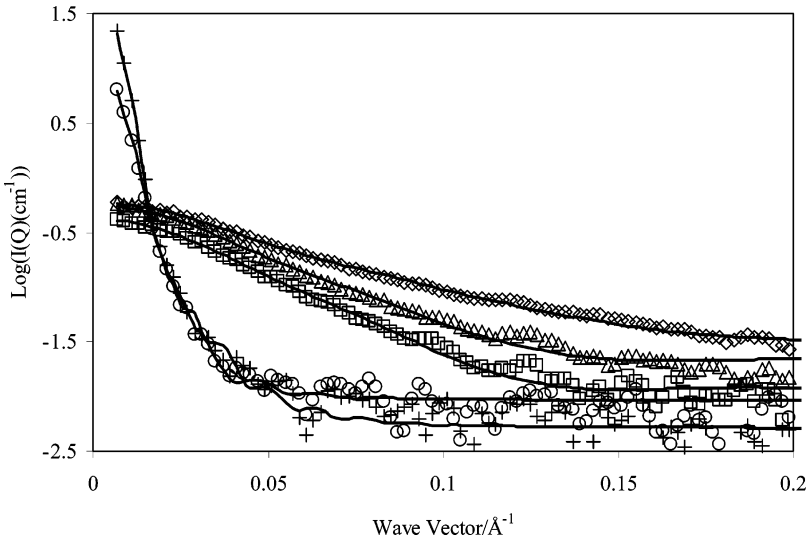

Figure 3. SANS scattering intensity (*I*) plotted against wave vector (*q*) from 5 mg/mL pure copolymer (MPC30−DEA70) solution (◇); and polyplexes (MPC30−DEA70/ODN) solution at the N/P ratios (amine/phosphate) of 10:1 (△), 5:1 (□), 2:1 (+), and 0.8:1 (○). ODN concentrations were fixed at 0.5 mg/mL for each sample at pH 7. Symbols represent the scattering signals, while continuous lines represent the fitted curves.

Table 1. Best-Fit Parameters for the SANS Curves Shown in Figure 3[a]

N/P ratios	molecular ratios (copolymer:ODN)	scale factor	diameter (Å)	length (Å)
copolymer itself at 0.5 wt %		6.29×10^{-6}	30 ± 2	180 ± 30
10:1	2:1	1.32×10^{-6}	30 ± 2	180 ± 30
		1.47×10^{-6}	52 ± 2	180 ± 30
5:1	1:1	1.34×10^{-6}	52 ± 2	200 ± 30
2:1	1:2.5	5.15×10^{-6}	46 ± 2	1000 ± 100 or higher
1:1	1:5	2.80×10^{-6}	46 ± 2	1000 ± 100 or higher
0.8:1	1:6.3	2.01×10^{-6}	360 ± 15	1000 ± 100 or higher
0.6:1	1:8.3	1.52×10^{-6}	370 ± 15	1000 ± 100 or higher

[a] The scale factor was derived from the quantitative model fitting and had no obvious physical meaning.

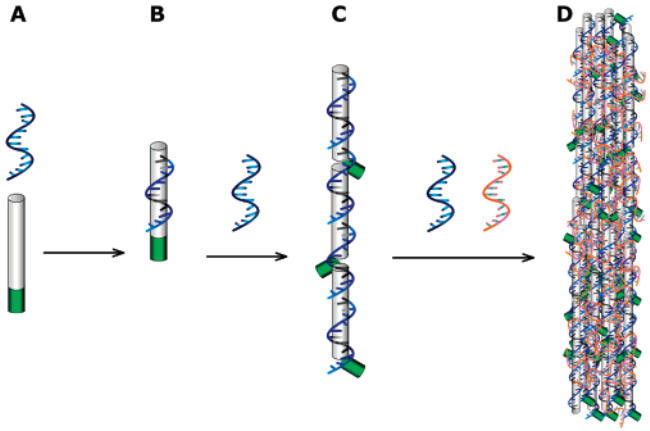

Figure 4. Schematic models to indicate the progressive binding of ODN onto copolymer to form polyplexes at different N/P ratios (gray cylinders for DEA blocks; green tails for MPC blocks). (A) ODN molecule and copolymer cylinder; (B) small polyplex at N/P ratios between 10/1 and 5/1; (C) small but long polyplex at N/P ratios between 2/1 and 1/1; (D) large polyplex at N/P ratios around 0.6/1.

its length did not change much, indicating that ODN molecules bound onto the copolymer molecules. As ODN was flexible (single stranded) and was much shorter than the copolymer, it must have bound around the copolymer to adopt its preferable helical configuration. The structural implication is schematically depicted in Figure 4A and B. Because the width of a single-stranded ODN was around 10 Å[40] and binding around the copolymer led to spiral pitches, the schematic description would account for some 20 Å increase in the cylindrical diameters of the complexes formed, consistent with the diameter increase. The persistence length of ODN is 2−3 nm,[41] so the elastic penalty for binding is not too large.

The N/P ratio of 10/1 is equivalent to the molar ratio of 2/1 with excess copolymer (for this copolymer the unit charge weight is about 310 g/mol and is almost the same as that for an average charge unit of ODN assuming that each amine group carries one cationic charge while each phosphate group carries one anionic charge[21]). This means that on average one-half of the copolymer molecules could be left free while the other one-half complexed with ODNs (note that ODN was much smaller). It was indeed found that the scattering profile from the polyplex solution at N/P = 10/1 could be well fitted to the coexistence of both types of cylinders in a 1:1 ratio, equivalent to polyplexes and excess copolymers with the same length but with different diameters (Table 1). For the polyplexes formed at N/P = 5/1 (molar ratio = 1/1), however, the neutron scattering profile could only be fitted to the polyplex cylinder model. It must be borne in mind that charge neutralization would produce polyplexes with a range of charge distribution at a given N/P ratio as revealed from DLS and gel electrophoresis. The good fits produced from the SANS models suggested that the extent of distributions was insufficient for SANS to detect any existence of free copolymers or the size distribution arising from different ODN binding.

Each ODN has 15 bases and is around 50 Å long.[40] In contrast, the full length of the DEA block is some 180 Å and is about 4 times longer. Taking into account the spiral

configuration, each DEA could accommodate 4 ODN molecules, assuming that ODN adopted the end-to-end binding surrounding the DEA in a single layer. However, local conformational restriction and mismatch in unit charge size and geometrical configuration would make this process less regular, and the situation would become worse as the ODN concentration was increased. Because electrostatic repulsion may prevent the overlapping of ODNs when wrapping around the copolymer, the single layer ODN binding was a reasonable assumption. Residual positive charges could remain due to incomplete neutralization. Our interfacial binding study has indicated that ODN molecules had no affinity to MPC blocks when the copolymers were preadsorbed at the silicon oxide/water interface (unpublished work). This was due to the zwitterionic character and strong hydration. It is thus assumed in this work that MPC did not interact with ODN.

The N/P ratios of 2/1 and 1/1 (lanes 4 and 5 in Figure 1) are equivalent to the molar ratios of 1/2.5 and 1/5 with ODN in excess. The SANS measurements revealed that, over this region, the cylindrical length increased substantially but their diameters changed little. This suggested that ODN binding helped to bridge the small polyplexes mainly through the end-to-end connection, resulting in extending their length as schematically shown in Figure 4C. Thus, all of the ODN molecules bound to copolymer backbones without causing cross-bundling, resulting in diameter increase. As already discussed, although SANS was less sensitive to the length change, its increase was well justified from the changes in scattering profiles measured.

As the N/P ratios were decreased to 0.8/1 and 0.6/1, the equivalent molar ratios became 1/6.3 and 1/8.3. The negatively charged ODNs were in further excess. Some of the excess ODN molecules appeared to bind across different polyplex cylinders under these conditions, forming new copolymer/ODN polyplexes with much larger diameters (Figure 4D) as evident from the SANS measurements. As this process of binding could hardly guarantee the full neutralization of the bound ODNs, some of the negative charges remained. Thus, the large polyplexes now carried net negative charges.

We have also undertaken AFM measurements by dropping a small amount of pure copolymer and polyplex solutions onto mica and bare hydrophilic silicon oxide, followed by rinsing with buffer and drying. The AFM imaging was carried out in isopropanol. Pure copolymers and polyplexes formed at high N/P ratios could not be visualized because they were too small, but large ones formed at N/P = 0.8/1 and 0.6/1 were easily identified (unpublished results). The shape and dimensions of these polyplexes were similar to those obtained from SANS under the same solution conditions. The AFM images thereby provided important verification to SANS data when large polyplexes were formed. Vinogradov et al.[9] have speculated that a number of initial smaller polyplexes could contribute to the formation of larger micelle-like aggregates. This hypothesis has been confirmed in our work. We note that many authors have examined structural changes relating to the complexation with large plasmid DNAs; for example, Chim et al.[20] have used AFM to examine the polyplexes formed between $MPC_{30}-DMA_x$ (where x is the mean degree of polymerization of the DMA block) and gWiz luc plasmid DNA and observed a range of sizes and shapes depending on the copolymer structure, N/P ratio, etc. However, complexation between polymer and plasmid, where the latter is significantly larger, proceeds by a different mechanism. We defer the discussion to a later stage. It is nevertheless useful to note that Chim et al.[20] observed rod and rectangular block-like structures for $x = 60$ under excess DNA charges, consistent with the finding from our system. Wittmar et al.[42] also showed rod-like condensed DMA/plasmid DNA (pBR322) polyplexes from AFM imaging. As indicated previously, Hodrien et al.[38] also observed a hydrodynamic size increase when excess double-stranded DNAs bound onto the cationically charged polystyrene particles. While the SANS measurement is consistent with most literature findings under excess DNA, its high sensitivity has revealed that ODN binding underwent two stages, the initial binding around the copolymer backbone chain and the end-to-end bridging to the charge ratio close to 1:1, and the subsequent cross-bundling when ODN is in excess. Measurement of hydrodynamic diameter by DLS alone could not reveal this process of structural transition.

Cell Transfection by Copolymer/ODN Polyplexes. Cell transfection experiments were carried out in parallel with the physical characterization using different polyplexes formed, and typical micrographs are shown in Figure 5. Transfection efficiencies relative to the total number of cells in each culture condition are shown in Figure 6. The positive control by Oligofectamine achieved a high transfection efficiency (over 95%), while the negative control (ODN alone) resulted in almost no transfection. Transfection efficiencies at N/P ratio = 10/1 and 5/1 appeared to be similar, and more than 95% of cells were transfected. In both cases, strong fluorescence from each cell was observed. The transfection efficiency decreased to 60−90%. Lowering the N/P ratio to below 1 resulted in even lower transfection efficiency.

These results correlated well with the widely reported charge effect: transfection efficiency decreases with decreasing positive charge density on the polyplexes. This decreasing trend of transfection also follows the size increase for the polyplexes, making it difficult to ascertain if size change has any role at all. Over the low N/P ratio range where ODN charges were in excess, the excess ODNs were not complexed. This together with increasing polyplex size meant that the number of complexes was also significantly reduced. Thus, all three factors (net charge, size, and number) were in fact related, and they together contributed to the observed drop in transfection efficiency with decreasing N/P ratio.

The transfection efficiency shown in Figure 6 illustrates strong transfection in the presence of FBS, indicating the stability of the polyplexes in serum. In the absence of FBS, toxicities became high with copolymer concentration. The transfection efficiency was also slightly lower in the absence of 10% FBS. These findings are in contrast to the data obtained for ODN intracellular delivery by most cationic lipid vectors where the presence of serum tends to reduce the transfection.[7,8,13] Another interesting observation from Figure 6 is that when the N/P ratio is below 5, there is an approximate but clear trend of linear decline of transfection efficiency against decreasing copolymer concentration. This is broadly true with and without the FBS given the large range of experimental errors. This observation would seem to indicate that it is the free copolymer concentration that matters. However, the charge initiated complexation and the associated structural changes of the polyplexes mean that such behavior is only nominal and that the actual mechanistic process is more complex.

To locate the ODN molecules inside the cell, a confocal laser scanning microscopy (CLSM) study of intracellular uptake and distribution of the ODNs in the transfected HeLa cells was performed, with select images displayed in Figure 7. Blue and green colors represent the respective DAPI stained nuclei and FAM fluorescence of ODNs scanned from the cells placed on a glass slide. From these images, we speculate that most of the

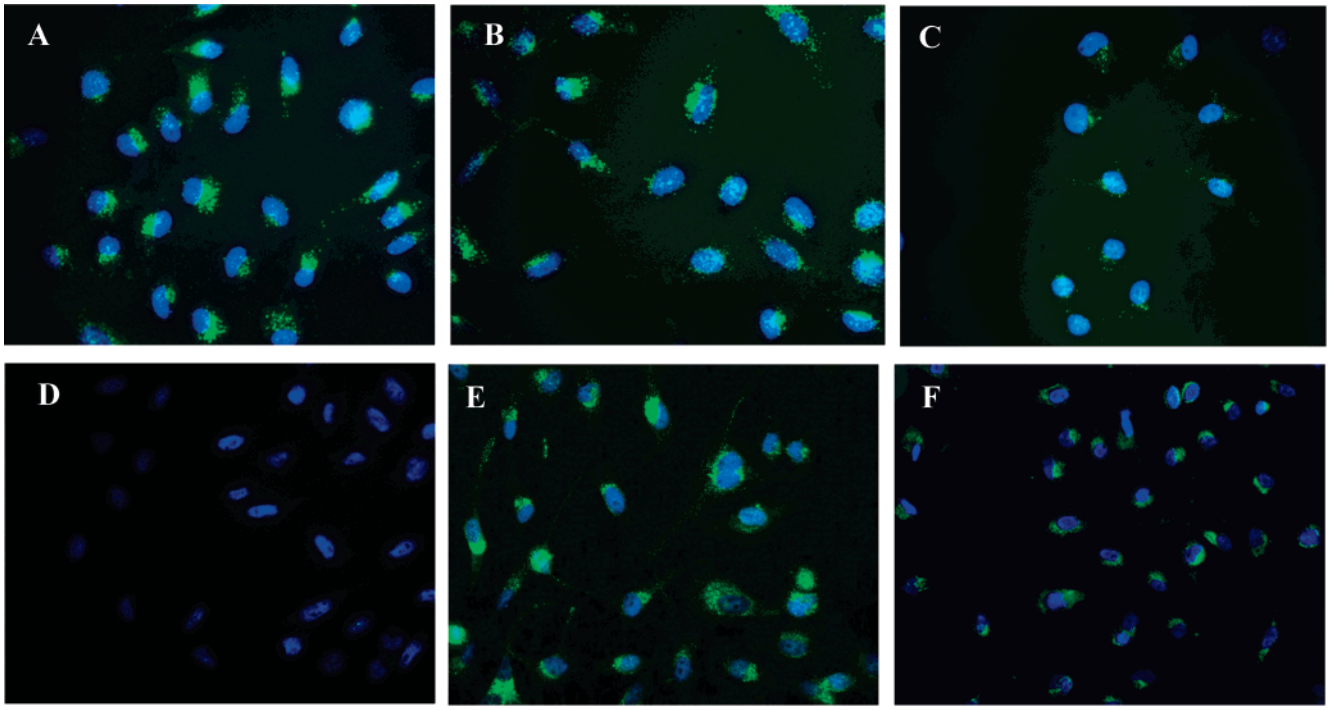

Figure 5. Images of HeLa transfection by copolymer/ODN polyplexes at different N/P ratios (A, 10:1; B, 2:1; C, 1:1; D, ODNs only; E, Oligofectamine/ODN = 3:1 as positive control; F, 5:1 using Hostasol-labeled copolymer and ODN (without any labeling)). Images were taken after 24 h transfection with 10% FBS. Blue color represents the cell nucleus by DAPI stain; green represents FAM fluorescence of ODN (green in (F) represents Hostasol-labeled copolymer).

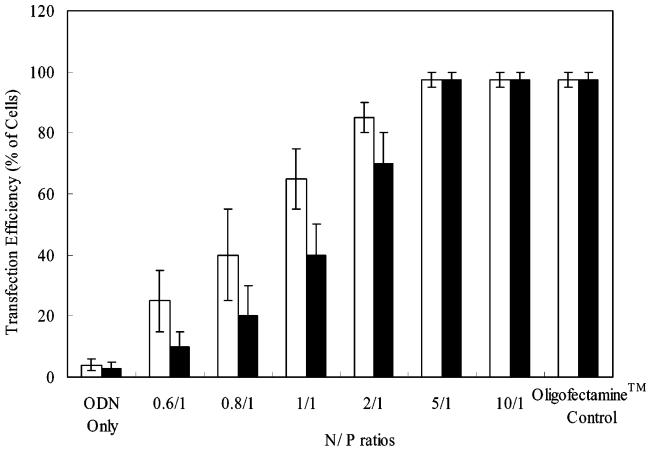

Figure 6. Transfection efficiency by ODN itself, copolymer/ODN polyplexes at different N/P ratios, and Oligofectamine/ODN complexes (positive control) with 10% FBS (white column) and without 10% FBS (black column).

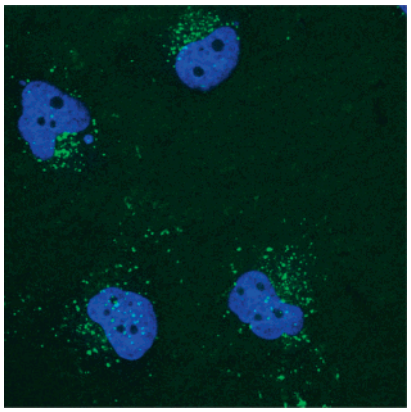

Figure 7. Confocal laser scanning microscopy (CLSM) study of intracellular uptake and distribution of the copolymer/ODN polyplexes in transfected HeLa cells. The blue color represents the cell nucleus stained by DAPI, while the green color represents the FAM fluorescence of ODNs.

ODN molecules engulfed by cells are located in and around the cell nuclei. In a parallel experiment using green fluorophore Hostasol tagged to the MPC block of the copolymer, it was found that there was a relatively high concentration of the copolymer surrounding the cell nuclei (Figure 5F). This observation did not rule out the presence of the copolymer in other regions of the cell, but if it was there, its concentration was relatively low. These experiments thus revealed the presence of ODN inside nuclei while the copolymers remained at the boundary region and were largely outside. From a similar CLSM study, Sirsi et al.[11] have also shown the translocation of their ODN molecules into myonuclei, while the copolymers (rhodamine-labeled PEI tagged with PEO) were almost completely excluded from entering the nuclei. Lucas et al.[12] have shown that, unlike low molar mass Cy5-labeled poly(L-lysine) (Cy5-pLL), high molar mass Cy5-*graft*-PDMA (1700 kDa) cannot enter the nuclei after microinjection in the cytoplasm. These authors further suggested that Cy5-pLL and ODNs were dissociated when the ODNs were internalized, although the precise location and timing of this dissociation were uncertain. Although delivery of ODNs to the nuclei has been emphasized in many reports, it might be unnecessary because the ODNs could bind to the target mRNA either in the nucleus as it is being formed and processed or in the cytoplasm when it is mature.[43]

The advantage of SANS is that it reveals the detailed structural progression of binding of ODN molecules to the much larger MPC30−DEA70 copolymers. The SANS results indicate that the initial binding of ODNs into the copolymers did not cause any association between copolymers. As the copolymer concentration was reduced, the ODN concentration effectively became high. Bridging occurred through end-to-end binding between copolymers, evident from the increase in the length of the small complexes but not in the diameter.[44] The substantial

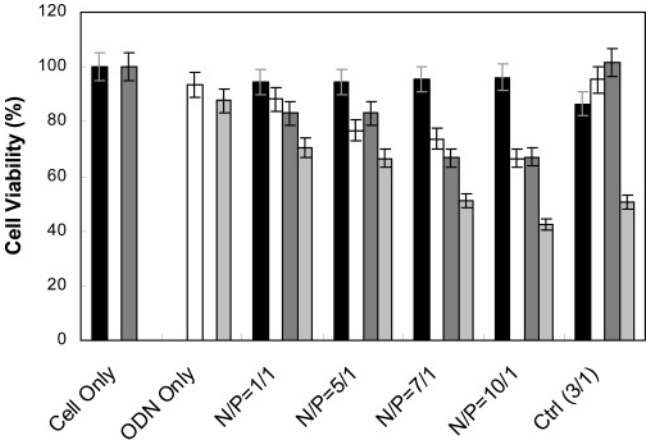

Figure 8. MTT assay of HeLa cell growth inhibition by copolymer/ODN polyplexes after 24 h incubation. The cell only and ODN only are used as references and negative controls with Oligofectamine/ODN = 3:1 as positive controls. Black (with 10% FBS) and gray (without FBS) columns are the cell viabilities references under different amounts of copolymer or Oligofectamine reagent equivalent to the dosages used for ODN complexes. White (with 10% FBS) and light gray (without FBS) columns are the cell viabilities under different N/P ratios of copolymer/ODN or Oligofectamine/ODN complexes (Ctrl). The dosages of ODN were all fixed at 0.1 μg/well in a 96-well plate with variable amount of copolymer.

length increase happened over the molar ratio between 1/2.5 and 1/5 with ODN in excess (the corresponding charge ratio dropped from net positive to overall neutral), overlapping with the full single layer binding predicted from the simple length argument as depicted previously. A further decrease in copolymer concentration led to the overall negative charges in the system, and the excess ODNs started forming physical cross-links that bundled the small polyplexes together to form larger ones. Thus, with increasing size of the polyplexes, the number of polyplexes dropped sharply and the charge density went from positive to negative.[45] In this regard, polyplex number and size must make important contributions to the changing transfection efficiency observed even if the apparent and crude linear relationship holds between transfection efficiency and copolymer concentration as depicted in Figure 6.

It is important to realize that the observed polyplex size and the number changes with N/P ratio should occur for systems where DNA is very small. A different mechanistic process is expected to occur with the complexation of long DNA chains. DNA plasmids normally contain some 5000 double-stranded base pairs and are significantly greater than the condensing cationic polymers. Although binding helps neutralize the charge and condense the DNA, its overall size after condensation is still substantial. Changes in charge sign and density are expected to play the dominant role, while size and shape changes are likely to be less significant. Thus, the two binding mechanistic processes are different. Design of the molecular size and architecture of the polymer vector for short DNA complexation should aim at achieving high proportion of positively charged polyplexes while keeping the size and number of the polyplexes under control.

Figure 8 shows the MTT assay that reveals the effect of cell growth inhibition by copolymer/ODN polyplexes. Simple ODN addition resulted in negligible cell growth inhibition as expected. Oligofectamine/ODN complexes showed no inhibition effect under 10% FBS, but 50% of cell growth inhibition was observed without FBS. In contrast, copolymer/ODN polyplexes show a clear trend of increasing inhibition with increasing N/P ratios, with and without FBS, confirming the serum stability of the copolymer/ODN polyplexes. At N/P ratio = 10/1, the inhibition reached some 30% and was clearly more effective than Oligofectamine in the presence of FBS. In the absence of FBS, Oligofectamine appeared to be slightly better. Serum stability and the cell growth inhibition observed indicated the hydrophilic shielding and stabilizing effect from the PC blocks in resemblance to that widely reported for cationic copolymers containing PEO blocks, showing the promising benefit of cationic MPC copolymers as non-viral gene transfecting vectors.

Cationic methacrylate-based copolymers such as those containing poly(2-dimethylamino ethyl) methacrylate (DMA) have also been used as transfecting vectors for different genes.[5−16,46,47] Most of these vectors contain hydrophilic PEO blocks. As in the case of PEI, the high transfecting efficiencies observed have been attributed to the strong buffering capacity under the physiological pH conditions. The buffering inside the endosomes due to the transfected polycations pumps protons into the endosomes (proton sponge effect) together with influx of anions to retain electroneutrality,[5−16] causing an increase in the local ionic strength. This process destabilizes the endosome, resulting in the escape of the gene complexes from the degradation inside the lysosomal environment. While the same proton sponge effect is expected to work in the case of MPC30−DEA70, the use of well-defined DMA or DEA copolymers avoids the complication from the chemical structures as often encountered in PEI copolymers and enables an easier establishment of the relationship between the nanostructure and charge density of the polyplexes formed and the subsequent transfection efficiency and cytotoxicity.

Gebhart et al.[48] and Ochietti et al.[49,50] have reported that, in addition to the attachment of a hydrophilic block to a cationic polymeric block to form polymeric vectors, grafting of a hydrophobic polymeric block such as poly(propylene) (PPO) in the form of PEO−PPO−PEO (Pluronic) to cationic PEI block can lead to the enhancement of transfection efficiency and control of favorable biodistribution of the complexes in animal models. They have further demonstrated that similar improvements can also be achieved by adding non-grafted Pluronic triblock copolymers. They suggested that by tuning the amphiphilicity of copolymers the binding with gene molecules can be made more effective, resulting in a favorable size range of the nanopolyplexes. A change of the ethyl group in a DEA block to methyl (DMA) and isopropyl group (DPA) represents a more effective control of amphiphilicity in the MPC copolymers.[51] This together with the variation of block size will enable us to examine the effect of hydrophobic interaction on the nanostructure and net charge density of the ODN polyplexes. The link of such information with cell transfection and cytotoxicity will be studied in future work.

Conclusions

We have combined electrophoresis, DLS, and SANS to characterize the size, shape, and charge characteristics of diblock copolymer/ODN polyplexes formed at different N/P ratios and found that changes in cell transfection efficiency resulted from a combined effect of polyplex charge, size, and number over the N/P range studied. In the systems reported here, ODN is significantly smaller than the polymeric vector, and the binding occurs in a different mechanistic process from the more widely studied systems where DNAs are much larger than the condensing vectors and the relative size changes during complexation are small.

SANS study revealed that the pure copolymer adopted a cylindrical conformation in the dilute aqueous solution, con-

sistent with a relatively rigid poly(methyl methacrylate) backbone with charged and zwitterionic side chains. The results indicated the existence of molecular solution of the copolymer with no indication of self-aggregation. The precise dimensions fitted indicated that the individual copolymers were fairly stretched and were not in the form of randomly coiled globule.

The ODN binding was driven by electrostatic interaction. It was found that, at high N/P ratios (with net positive charges), a few ODNs bound to each copolymer and there was no sign of polymer−polymer association caused by ODN binding. The nanocylindrical polyplexes carried net positive charges and had a similar size and shape to the free copolymers. While the strong cell transfection from these small nanocylinders benefited primarily from the charge, the absence of polymer association meant that the number of polyplexes was at the highest possible. As the N/P ratio approached unity, the SANS study revealed that the diameters of the polyplexes remained unchanged but that their lengths were increased substantially, suggesting that binding primarily occurred around individual copolymers leading to end-to-end bridging between copolymers. A further decrease in N/P ratio below 1 (with ODN in excess) initiated cross-bundling to form larger cylindrical polyplexes with increased diameters. As some of the ODN molecules bound were not fully neutralized, the large polyplexes carried net negative charges. Cross-bundling reduced the polyplex numbers. This together with the increasing net negative charges was consistent with the reduced transfection efficiency and fluorescence signal observed.

Cell growth inhibition assays showed that the MPC-based copolymers had low cytotoxicity to HeLa cells over the effective transfection dosage range and that ODN complexes formed from the copolymer outperformed those formed from commercial Oligofectamine in the presence of FBS. CLSM studies provided strong evidence for internalization of the ODNs into the cell nuclei. This study shows that the diblock copolymer MPC30−DEA70 can work as an effective, water-based ODN transfecting vector.

Acknowledgment. We would like to thank EPSRC, Impact Faraday Partnerships, and Biocompatibles UK Ltd. for their financial support under the grant GR/R90437/1. S.P.A. is the recipient of a Royal Society Wolfson Research Merit Award.

References and Notes

(1) Pack, D. W.; Hoffman, A. S.; Pun, S.; Stayton, P. S. Design and development of polymers for gene delivery. *Nat. Rev. Drug Discovery* **2005**, *4*, 581−593.
(2) Mehier-Humbert, S.; Guy, R. H. Physical methods for gene transfer: Improving the kinetics of gene delivery into cells. *Adv. Drug Delivery Rev.* **2005**, *57*, 733−753.
(3) Goverdhana, S.; Puntel, M.; Xiong, W.; Zirger, J. M.; Barcia, C.; Curtin, J. F.; Soffer, E. B.; Mondkar, S.; King, G. D.; Hu, J.; Sciascia, S. A.; Candolfi, M.; Greengold, D. S.; Lowenstein, P. R.; Castro, M. G. Regulatable gene expression systems for gene therapy applications: Progress and future challenges. *Mol. Ther.* **2005**, *12*, 189−211.
(4) Li, S.; Huang, L. Nonviral gene therapy: Promises and challenges. *Gene Ther.* **2000**, *7*, 31−34.
(5) Dias, N.; Stein, C. A. Antisense oligonucleotides: Basic concepts and mechanisms. *Mol. Cancer Ther.* **2002**, *1*, 347−355.
(6) Sarkar, T.; Conwell, C. C.; Harvey, L. C.; Santai, C. T.; Hud, N. V. Condensation of oligonucleotides assembled into nicked and gapped duplexes: potential structures for oligonucleotide delivery. *Nucleic Acids Res.* **2005**, *33*, 143−151.
(7) Garcia-Chaumont, C.; Seksek, O.; Grzybowska, J.; Borowski, E.; Bolard, J. Delivery systems for antisense oligonucleotides. *Pharmacol. Ther.* **2000**, *87*, 255−277.
(8) Yoo, H.; Juliano, R. L. Enhanced delivery of antisense oligonucleotides with fluorophore-conjugated PAMAM dendrimers. *Nucleic Acids Res.* **2000**, *28*, 4225−4231.
(9) Vinogradov, S. V.; Batrakova, E. V.; Li, S.; Kabanov, A. V. Mixed polymer micelles of amphiphilic and cationic copolymers for delivery of antisense oligonucleotides. *J. Drug Targeting* **2004**, *12*, 517−526.
(10) Brus, C.; Petersen, H.; Aigner, A.; Czubayko, F.; Kissel, T. Physicochemical and biological characterization of polyethylenimine-*graft*-poly(ethylene glycol) block copolymers as a delivery system for oligonucleotides and ribozymes. *Bioconjugate Chem.* **2004**, *15*, 677−684.
(11) Sirsi, S. R.; Williams, J. H.; Lutz, G. J. Poly(ethylene imine)−poly(ethylene glycol) copolymers facilitate efficient delivery of antisense oligonucleotides to nuclei of mature muscle cells of mdx mice. *Hum. Gene Ther.* **2005**, *16*, 1307−1317.
(12) Lucas, B.; Remaut, K.; Sanders, N. N.; Braeckmans, K.; Smedt, S. C. D.; Demeester, J. Studying the intracellular dissociation of polymer-oligonucleotide complexes by dual color fluorescence fluctuation spectroscopy and confocal imaging. *Biochemistry* **2005**, *44*, 9905−9912.
(13) Wilson, A.; Zhou, W.; Champion, H. C.; Alber, S.; Tang, Z.-L.; Kennel, S.; Watkins, S.; Huang, L.; Pitt, B.; Li, S. Targeted delivery of oligodeoxynucleotides to mouse lung endothelial cells in vitro and in vivo. *Mol. Ther.* **2005**, *12*, 510−518.
(14) Anderson, D. G.; Akinc, A.; Hossain, N.; Langer, R. Structure/property studies of polymeric gene delivery using a library of poly(B-amino esters). *Mol. Ther.* **2005**, *11*, 426−434.
(15) Putnam, D.; Gentry, C. A.; Pack, D. W.; Langer, R. Polymer-based gene delivery with low cytotoxicity by a unique balance of side-chain termini. *Proc. Natl. Acad. Sci. U.S.A.* **2001**, *98*, 1200−1205.
(16) Jessel, N.; Oulad-Abdelghani, M.; Meyer, F.; Lavalle, P.; Haîkel, Y.; Schaaf, P.; Voegel, J.-C. Multiple and time-scheduled in situ DNA delivery mediated by β-cyclodextrin embedded in a polyelectrolyte multilayer. *Proc. Natl. Acad. Sci. U.S.A.* **2006**, *103*, 8618−8621.
(17) Bromberg, L.; Alakhov, V. Y.; Hatton, T. A. Self-assembling Pluronic-modified polycations in gene delivery. *Curr. Opin. Colloid Interface Sci.* **2006**, *11*, 217−223.
(18) Merdan, T.; Kopecek, J.; Kissel, T. Prospects for cationic polymers in gene and oligonucleotide therapy against cancer. *Adv. Drug Delivery Rev.* **2002**, *54*, 715−758.
(19) Azzam, T.; Domb, A. J. Current developments in gene transfection agents. *Curr. Drug Delivery* **2004**, *1*, 165−193.
(20) Chim, Y. T. A.; Lam, J. K. W.; Ma, Y.; Armes, S. P.; Lewis, A. L.; Roberts, C. J.; Stolnik, S.; Tendler, S. J. B.; Davies, M. C. Structural study of DNA condensation induced by novel phosphorylcholine-based copolymers for gene delivery and relevance to DNA protection. *Langmuir* **2005**, *21*, 3591−3598.
(21) Zhao, X.; Zhang, Z.; Pan, F.; Ma, Y.; Armes, S. P.; Lewis, A. L.; Lu, J. R. Solution pH regulated interfacial adsorption of diblock phosphorylcholine copolymers. *Langmuir* **2005**, *21*, 9597−9603.
(22) Tang, Y.; Lu, J. R.; Lewis, A. L.; Vick, T. A.; Stratford, P. W. Structural effects on swelling of thin phosphorylcholine polymer films. *Macromolecules* **2002**, *35*, 3955−3964.
(23) Tang, Y.; Su, T. J.; Armstrong, J.; Lu, J. R.; Lewis, A. L.; Vick, T. A.; Stratford, P. W.; Heenan, R. K.; Penford, J. Interfacial structure of phosphorylcholine incorporated biocompatible polymer films. *Macromolecules* **2003**, *36*, 8440−8448.
(24) Dean, N. M.; Bennett, C. F. Antisense oligonucleotide-based therapeutics for cancer. *Oncogene* **2003**, *22*, 9087−9096.
(25) Crooke, S. T. Progress in antisense technology. *Annu. Rev. Med.* **2004**, *55*, 61−95.
(26) Pirollo, K. F.; Rait, A.; Sleer, L. S.; Chang, E. H. Antisense therapeutics: from theory to clinical practice. *Pharmacol. Ther.* **2003**, *99*, 55−77.
(27) Morris, M. C.; Vidal, P.; Chaloin, L.; Heitz, F.; Divita, G. A new peptide vector for efficient delivery of oligonucleotides into mammalian cells. *Nucleic Acids Res.* **1997**, *25*, 2730−2736.
(28) Shi, F.; Nomden, A.; Oberle, V.; Engberts, J. B. F. N.; Hoekstra, D. Efficient cationic lipid-mediated delivery of antisense oligonucleotides into eukaryotic cells: down-regulation of the corticotropin-releasing factor receptor. *Nucleic Acids Res.* **2001**, *29*, 2079−2087.
(29) Pulkkanen, K. J.; Yla-Herttuala, S. Gene therapy for malignant glioma: Current clinical status. *Mol. Ther.* **2005**, *12*, 585−598.
(30) Kutryk, M. J. B.; Foley, D. P.; Brand, M. v. d.; Hamburger, J. N.; Giessen, W. J. v. d.; deFeyter, P. J.; Bruining, N.; Sabate, M.; Serruys, P. W. Local intracoronary administration of antisense oligonucleotide against c-myc for the prevention of in-stent restenosis. *J. Am. Coll. Cardiol.* **2002**, *39*, 281−287.
(31) Stein, C. A. The experimental use of antisense oligonucleotides: a guide for the perplexed. *J. Clin. Invest.* **2001**, *108*, 641−644.

(32) Smedt, S. C. D.; Remaut, K.; Lucas, B.; Braeckmans, K.; Sanders, N. N.; Demeester, J. Studying biophysical barriers to DNA delivery by advanced light microscopy. *Adv. Drug Delivery Rev.* **2005**, *57*, 191−210.
(33) Elouahabi, A.; Ruysschaert, J.-M. Formation and intracellular trafficking of lipoplexes and polyplexes. *Mol. Ther.* **2005**, *11*, 336−347.
(34) Ma, Y.; Tang, Y.; Billingham, N. C.; Armes, S. P.; Lewis, A. L.; Lloyd, A. W.; Salvage, J. P. Well-defined biocompatible block copolymers via atom transfer radical polymerization of 2-methacryloyloxyethyl phosphorylcholine in protic media. *Macromolecules* **2003**, *36*, 3475−3484.
(35) Berne, B. J.; Percora, R. *Dynamic Light Scattering*; Wiley: New York, 1976.
(36) King, S. M. Small Angle Neutron Scattering. *Modern Techniques for Polymer Characterization*; Wiley & Sons Ltd.: New York, 1999; Chapter 7, pp 171−231.
(37) Zhang, Z.; Cao, X.; Zhao, X.; Withers, S. B.; Holt, C. M.; Lewis, A. L.; Lu, J. R. Controlled delivery of antisense oligodeoxynucleotide from cationically modified phosphorylcholine polymer films. *Biomacromolecules* **2006**, *7*, 784−791.
(38) Hodrien, A. J.; Waigh, T. A.; Voice, A. M.; Blair, G. E.; Clarke, S. M. Adsorption of DNA onto positively charged amidine colloidal spheres and the resultant bridging interaction. *Int. J. Biol. Macromol.* **2007**, *41*, 146−153.
(39) Waigh, T. A.; Ober, R.; Williams, C. E.; Galin, J. C. Semi-dilute solutions of a solvophobic polyelectrolyte in nonaqueous solvents. *Macromolecules* **2001**, *34*, 1973−1980.
(40) Nelson, D. L.; Cox, M. M. *Lehninger Principles of Biochemistry*, 4th ed.; W. H. Freeman and Co.: New York, 2005.
(41) Murphy, M. C.; Rasnik, I.; Cheng, W.; Lohman, T. M.; Ha, T. Probing single-stranded DNA conformational flexibility using fluorescence spectroscopy. *Biophys. J.* **2004**, *86*, 2530−2537.
(42) Wittmar, M.; Ellis, J. S.; Morell, F.; Unger, F.; Schumacher, J. C.; Roberts, C. J.; Tendler, S. J. B.; Davies, M. C.; Kissel, A. T. Biophysical and transfection studies of an amine-modified poly(vinyl alcohol) for gene delivery. *Bioconjugate Chem.* **2005**, *16*, 1390−1398.
(43) Roth, C. M.; Sundaram, S. Engineering synthetic vectors for improved DNA delivery: Insights from intracellular pathways. *Annu. Rev. Biomed. Eng.* **2004**, *6*, 397−426.
(44) Podgornik, R.; Ličer, M. Polyelectrolyte bridging interactions between charged macromolecules. *Curr. Opin. Colloid Interface Sci.* **2006**, *11*, 273−279.
(45) Grosberg, A. Y.; Nguyen, T. T.; Shklovskii, B. I. The physics of charge inversion in chemical and biological systems. *Rev. Mod. Phys.* **2002**, *74*, 329−345.
(46) Thomas, M.; Lu, J. J.; Ge, G.; Zhang, C.; Chen, J.; Klibanov, A. M. Full deacylation of polyethyleneimine dramatically boosts its gene delivery efficiency and specificity to mouse lung. *Proc. Natl. Acad. Sci. U.S.A.* **2005**, *102*, 5679−5684.
(47) van-de-Wetering, P.; Moret, E. E.; Schuurmans-Nieuwenbroek, N. M.; van-Steenbergen, M. J.; Hennink, W. E. Structure-activity relationships of water-soluble cationic methacrylate/methacrylamide polymers for non-viral gene delivery. *Bioconjugate Chem.* **1999**, *10*, 589−597.
(48) Gebhart, C. L.; Sriadibhatla, S.; Vinogradov, S.; Lemieux, P.; Alkahov, V.; Kabanov, V. A. Design and formulation of polyplexes based on Pluronic-polyethyleneeimine conjugates for gene transfer. *Bioconjugate Chem.* **2002**, *13*, 937−944.
(49) Ochietti, B.; Guerin, N.; Vinogradov, S. V.; St-Pierre, Y.; Lemieux, P.; Kabanov, A. V.; Alakhov, V. Y. Altered organ accumulation of oligonucleotides using polyethyleneimine grafted with poly(ethylene oxide) or Pluronic as carriers. *J. Drug Targeting* **2002**, *2*, 113−121.
(50) Ochietti, B.; Lemieux, P.; Kabanov, A. V.; Vinogradov, S.; St-Pierre, Y.; Alakhov, V. Inducing neutrophil recruitment in the liver of ICAM-1. *Gene Ther.* **2002**, *14*, 939−945.
(51) Lobb, E. J.; Ma, I.; Billingham, N. C.; Armes, S. P.; Lewis, A. L. Facile synthesis of well-defined, biocompatible phosphorylcholine-based methacrylate copolymers via atom transfer radical polymerization at 20 °C. *J. Am. Chem. Soc.* **2001**, *123*, 7913−7914.

BM7006482